Modeling with COMSOL the Interaction between Subducting Plates and Mantle Flow

J. Rodríguez-González[1*], A. M. Negredo[1], P. Petricca[2], E. Carminati[2,3]
[1] Departamento de Geofísica y Meteorología, Facultad de CC. Físicas, Universidad Complutense de Madrid, Av. Complutense s/n, 28040 Madrid, Spain
[2]Dipartimento di Scienze della Terra, Università di Roma "La Sapienza", Roma, Italy
[3]Istituto Geologia ambientale e Geoingegneria – CNR, Roma, Italy
* juan.rodriguez@fis.ucm.es

Abstract: Subduction processes have great importance as are related to volcanism and earthquake occurrence. Old and cold plates should subduct steeper than younger ones, but the subduction angle is highly variable and does not always correlate with the age of the plates.
Some researchers propose a global or net westward drift of the lithosphere relative to the mantle and this assessment is still a matter of debate. Geophysical evidence suggests that polarity of the subduction could affect the angle of subduction.
The relative motion between lithosphere and underlying mantle would affect the geometry of subduction. We have run several simulations in which a horizontal flux has been imposed on the sublithospheric mantle to test its effect. In the shallower part of the slab the angular difference is small but it has greater effect on the deeper region and in some cases it inhibits the penetration of the slab into the lower mantle.

Keywords: Physical and numerical modeling, subduction, asthenospheric horizontal flux.

1. Introduction

Slab dips vary significantly both in different and along single subduction zones (Isacks and Barazangi, 1977; Jarrard, 1986; Cruciani et al., 2005; Lallemand et al., 2007). Such variations have been investigated and explained to be either 1) the result of a balance between the downward torque on the slab due to the weight of the slab and the upward torque exerted by hydrodynamic forces from the induced corner flow in the viscous mantle wedge (Stevenson and Turner, 1977; Tovish et al., 1978) or 2) the effect of the return flow of the mantle produced by the plate motion rather than by slab density contrasts (Hager and O'Connell, 1978). A long lasting and popular idea is that slab pull controls slab dynamics, i.e., cooler subducting lithosphere is heavier than the surrounding mantle and sinks passively. A corollary is that, since buoyancy of the slab is proportional to its age, the dip of slabs composed of younger seafloor would be smaller (Wortel and Vlaar, 1978; Barazangi and Isacks, 1979; Jordan et al., 1983).
However, this simple scenario is sometimes at odds with observations that provide noticeable exceptions, such as the steep subduction of a young slab along the Sandwich subduction zone or the more flatten subduction of an old slab in the Indonesian subduction zone.
Assuming that hotspots can be taken as a fixed reference frame (e.g., Norton, 2000), hotspot tracks clearly indicate a relative motion between lithosphere and the underlying mantle, the asthenosphere acting as a detachment layer due to its low viscosity. Several researchers proposed a global or net westward drift of the lithosphere relative to the mantle (e.g., Bostrom, 1971; Gripp and Gordon, 2002; Cuffaro and Jurdy, 2006), with average rates between 4.9 cm/yr (Gripp and Gordon, 2002) and 13.4 cm/yr (Crespi et al., 2007). This westward drift has been considered to be an average motion of the lithosphere, due to the larger weight of the Pacific plate in the global plate-motion computation (e.g., Ricard et al., 1991). As an alternative, it has been proposed that all the plates display a westward drift with respect to the mantle (e.g., Doglioni et al., 1999). These alternative models derive from plate velocity reconstructions based on different hotspots reference frames. A debate recently arose regarding whether hotspots are deep or shallow features (Foulger et al., 2005). If hotspots are assumed to be of deep origin, some plates do move eastward with respect to the mantle (e.g., Gripp and Gordon 2002). If they are shallow sourced, then all the plates move westward (e.g., Cuffaro and Doglioni 2007). The definition of a proper reference frame and the consequent calculation of plate motions are beyond the scope

of this work. However, it is clear that, owing to the dip direction of the slab with respect to the absolute plate motion, slabs may either oppose or accompany the relative mantle flow.
Geological and geophysical observations suggest that the polarity of subduction zones and the relative motion of the subducting plate with respect to the mantle strongly control the characters of subduction-related orogens and slab dips (e.g., Doglioni et al., 1999). However, no consensus has been reached on this issue (e.g., Cruciani et al., 2005 vs. Lallemand et al., 2005). The controversy is due to some major problems: 1) the data sets used to measure actual dips of slabs are not uniform; 2) the effects of absolute plates motions on slab dips are summed to those of the other factors described above and are not easily extractable from data; 3) no agreement has been reached on the reference frame (and therefore on the resulting velocities).
The influence of the relative motion of the lithosphere with respect to the mantle has not been tested quantitatively. In this work we address this subject simulating with 2D numerical models the dynamic evolution of subduction zones. Rather than addressing a specific region, we investigate the physics of the process varying calculation parameters (such as the plate age, the plate convergence and the relative mantle velocity) and show that indeed the mantle flow influences the slab geometry.

2. Model setup and numerical method

2.1 Governing equations

The model domain represents a vertical section running parallel to the subduction direction, in which equations of conservation of mass, momentum and energy are solved for an incompressible 2-D fluid:

$$\nabla\vec{\mathbf{u}} = 0$$

$$\rho\frac{\partial\vec{u}}{\partial t} - \nabla[\eta(\nabla\vec{u} + (\nabla\vec{u})^T)] + \rho(\overrightarrow{u\nabla})\vec{u} + \nabla P = \vec{F}$$

$$\rho C_P\left(\frac{\partial T}{\partial t} + \vec{u}\nabla T\right) - \nabla(\kappa\nabla T) = Q$$

Where $\vec{u}$ is the fluid velocity, P the pressure, C_p the specific heat, κ the thermal conductivity, η the viscosity, the term it multiplies is the stress tensor, and ρ the density. The term on the right side of (2) includes all the body forces acting on the fluid, and in this model we only include the gravity force. The term Q on the right side of (3) contains heat sources.
The incompressibility hypothesis, strictly applied, implies the assumption of a uniform density and this would cancel all the buoyancy forces. Instead, we use the *extended Boussinesq approximation* and assume that density variations are considered only when related to buoyancy forces and take into account thermal effects due to pressure changes (e.g. Tritton, 1988). Therefore we calculate heat release (absorbed) through adiabatic upwelling (downwelling) as the only source of heat, using the expression $Q_{ad}=-\rho\alpha g v_y T$, where α is the thermal expansion coefficient, v_y is the vertical component of the velocity. Here we have considered only density variations due to temperature following the simplified state equation: $\rho=\rho_0(1-\alpha T)$, where, ρ_0 is the density at 0°C.

2.2 Rheology

We use a viscosity law given by Hirth and Kohlstedt (2003):

$$\eta_{df,dis} = \left(\frac{d^p}{AC_{OH}{}^r}\right)^{1/n} \dot{\varepsilon_{II}}^{\frac{1-n}{n}} exp\left[\frac{E + P_{lit}V}{nRT}\right]$$

Where d is the grain size, p the grain size exponent, A the pre-exponential factor, C_{OH} OH concentration, E and V activation energy and volume, P_{lit} the lithostatic pressure, R the gas constant, n the stress exponent and $\dot{\varepsilon}_{II} = (\dot{\varepsilon}_{ij}\dot{\varepsilon}_{ij})^{1/2}$ the *effective strain rate*. Therefore, if n=1, there is no dependence on the strain rate and a Newtonian rheology is reproduced.

2.3 Model setup

The modeled section is 1200 km deep and its width varies between 2500 and 5500 km (Fig. 1). It is a stratified model in which three different layers are established through three different initial temperature distributions: lithosphere, upper mantle and lower mantle.
Lithosphere extends from the surface to a depth of 95 km, and its thermal distribution follows the GDH1 plate model by Stein and Stein (1992).

$$T_{lit}(z,t') = T_L\left(\frac{z}{L} + \sum_{n=1}^{\infty}\frac{2}{n\pi}\sin\left(\frac{n\pi z}{L}\right)exp\left(\frac{-n^2\pi^2 Kt'}{\rho C_p L}\right)\right)$$

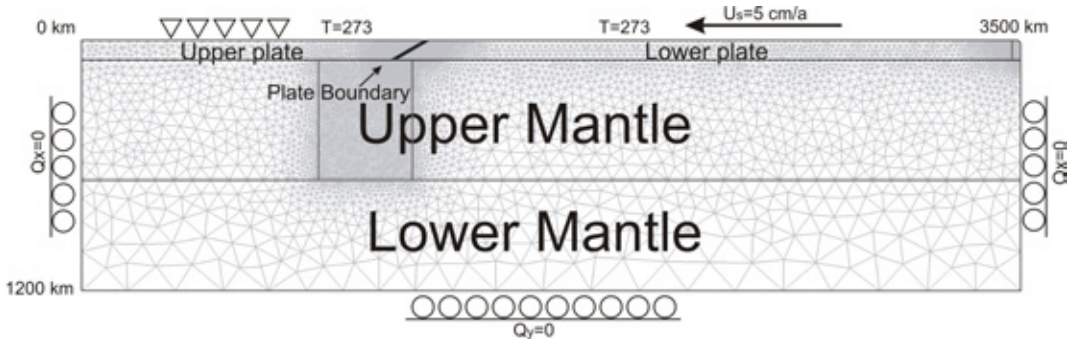

Figure 1: Schematic representation of the modeled vertical cross section showing mesh and boundary conditions of the reference model (without horizontal asthenospheric flow).

Where T_L=1450 ºC is the temperature at the base of the lithosphere and *t'* is the age of the plate. For the upper plate a uniform age is used, but the age of the lower plate increases with the distance to the right boundary, which represents an oceanic ridge. The age is then computed as t'=D/u_s, where *D* is the distance to the ridge and u_s=5 cm/yr is the subduction velocity. Provided that the rightmost edge of the model represents the oceanic ridge, we can vary the maximum age for the lower plate by varying the width of the modeled domain.

Both in the upper and lower mantle we impose an adiabatic distribution for the temperature:

$$T_m(z) = T_L exp\left[\frac{g\alpha}{C_p}(z-L)\right]$$

The upper boundary has a constant temperature of 0ºC. The top of the subducting plate has a constant velocity u_s=5 cm/yr to reproduce subduction and the upper boundary of the upper plate is fixed. The rest of the boundaries have a free slip condition and are thermally insulated in the reference model. To reproduce horizontal mantle flow, an inlet velocity is applied at one of the lateral boundaries, from 95 to 670 km depth, while the same outlet flux is imposed on the opposite boundary.

Finally, in order to reproduce subduction, we have imposed a narrow low viscosity region at the plate boundary. This low viscosity channel is intended to simulate a fault that decouples subducting and upper plates without producing singularities on the stress distribution (Billen and Hirth, 2007; Kukaeka and Matyska, 2004). Viscosity, shape, depth and width of the fault have great influence on the geometry of subduction (Jischke, 1975; Kinkaid and Sacks, 1997; Manea and Gurnis 2007). Therefore, we have chosen the parameters that best reproduce subduction: the low viscosity channel is 15 km wide and 95 km deep and has a dip of 30º and a maximum viscosity of 10^{22} Pa s. This model setup and the way to simulate the plate boundary and to reproduce subduction are very similar to modeling by Billen and Hirth (2005, 2007).

2.4. Numerical modeling

In these models the Navier-Stokes and the thermal equations are coupled due to the temperature dependence of ρ, η and to the advection term on the heat equations.

Therefore this is a multiphysics problem where we make use of two COMSOL modes: Incompressible Navier-Stokes (n.s.) and Heat Transfer (convection and conduction, c.c.). We use the velocity distribution obtained by the first mode in the second one and the temperature distribution obtained by c.c. mode on the n.s. one.

To achieve convergence during the transient analysis we first calculate the convergent solution to the n.s. mode using UMFPAK solver. We use this velocity field as initial velocity to obtain the initial viscosity of the transient state, performed with PARDISO solver.

We have used between 15000 and 30000 triangular mesh elements. The density of the mesh used along the model varies from one node every 2 km in the plate boundary area to one every 150 km on the lower mantle. This variability of element density allows us to deal with high viscosity contrasts, avoiding great computational requirements

3. Results and concluding remarks

We have tested the influence of an imposed flux on the sublithospheric mantle[1] for plates of different ages. We have run several simulations

[1] For simplicity, from now on we will refer to it as *Horizontal Asthenospheric Flux or HAF*.

in which we vary the sense of the flux (favoring or opposing subduction) and its velocity and compare them with a reference model without HAF.

3.1. Reference model

In the reference model the upper plate is 20 Myr old and the lower plate's maximum age is 40 Myr (Fig. 2). At the first stage of the evolution only one convective cell appears beneath the lower plate. While the simulation evolves, the lower plate bends downward and subduction begins (Fig 2.A). While the colder lower plate penetrates in the warmer mantle, the flux pattern changes and the material from the asthenosphere starts to flow in the wedge formed between the upper and the lower plate (*asthenospheric wedge*). At first the slab becomes increasingly steep due to the negative buoyancy force generated as a consequence of the temperature difference between the subducting plate and the asthenosphere. While the flux on the *asthenospheric wedge* becomes stronger, suction forces increase and the shallowest part of the slab flattens. Therefore, the angle of subduction decreases for the shallowest part (due to suction forces) and it increases at the deeper part (due to negative buoyancy).

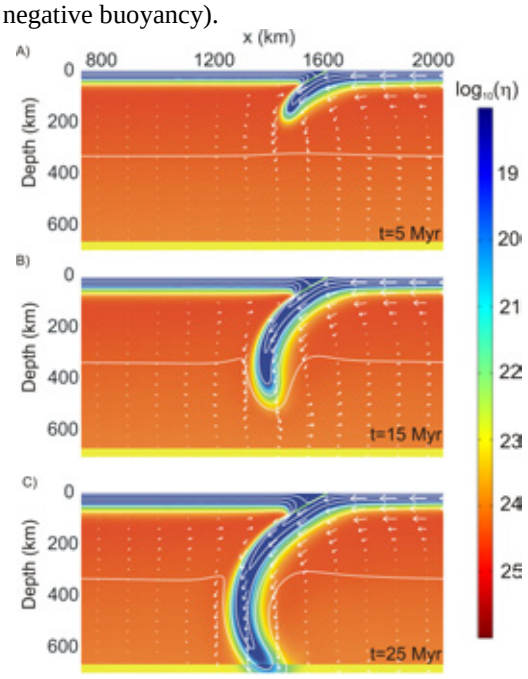

Figure 2: Evolution of the reference model after 5, 15 and 25 Myr. Reference model is characterized by a 20 Myr old upper plate and a 40 My old lower plate, by subduction velocity of 5 cm/yr, by Newtonian viscosity and by no HAF. Viscosity in logarithmic scale *(colormap) and contours of equal temperature every 280 degrees are shown.*

3.2. Influence of the horizontal flux

We show here the results of other four different simulations including the HAF: two in which the HAF is directed to the right and other two in which it is directed to the left[2]. We have tested two HAF velocities: 4 cm/yr and 8 cm /yr.

During the first stage of the evolution, there is no significant difference among all simulations (Fig. 3). Nevertheless, while the slab penetrates into the asthenosphere, the material of the sublithospheric mantle is channeled between the colder slab and the lower mantle (ten times more viscous than the overlaying material) and its velocity increases. The higher velocity and the increase in length of the slab tend to increase the effect of the flux as the model evolves (Fig. 3.A). Therefore, if the HAF is directed to the right the subduction the angle of subduction is higher, whreas the angle decreases when the HAF is directed to the left. The angular difference increases when the velocity imposed at the lateral boundaries is higher.

The angular difference also increases in the deeper parts of the slab (Fig. 3.B). Apart from the higher velocity found in this region, this part of the slab is distant from the trench, and the torque generated by the HAF is consequently higher.

One of the most important results is found when the slab is about to penetrate into the lower mantle. Whereas the slab penetrates into the lower mantle if there is no HAF (Fig. 4.B), this result is not reproduced in some simulations with HAF (Figs. 4.A and 4.C). When the channel is about to close, the velocity of the material channeled between the slab and the lower mantle is so high that the penetration into the lower mantle is inhibited. If the flux directed to the right, the slab bends backward and rests between the upper and the lower mantle. If the flux is directed to the left, in some cases, the dip of the slab is so low that it does not reach the lower mantle.

The simulations in which the plates have different ages reproduced similar results: the effect of the HAF is negligible during the first millions years and in the shallower parts of the slab while its effect is stronger for the deeper parts and in some cases it inhibits penetration into the lower mantle.

[2] The velocity of the HAF is positive when it faces subduction (HAF directed to the right) and negative when it has the opposite sense.

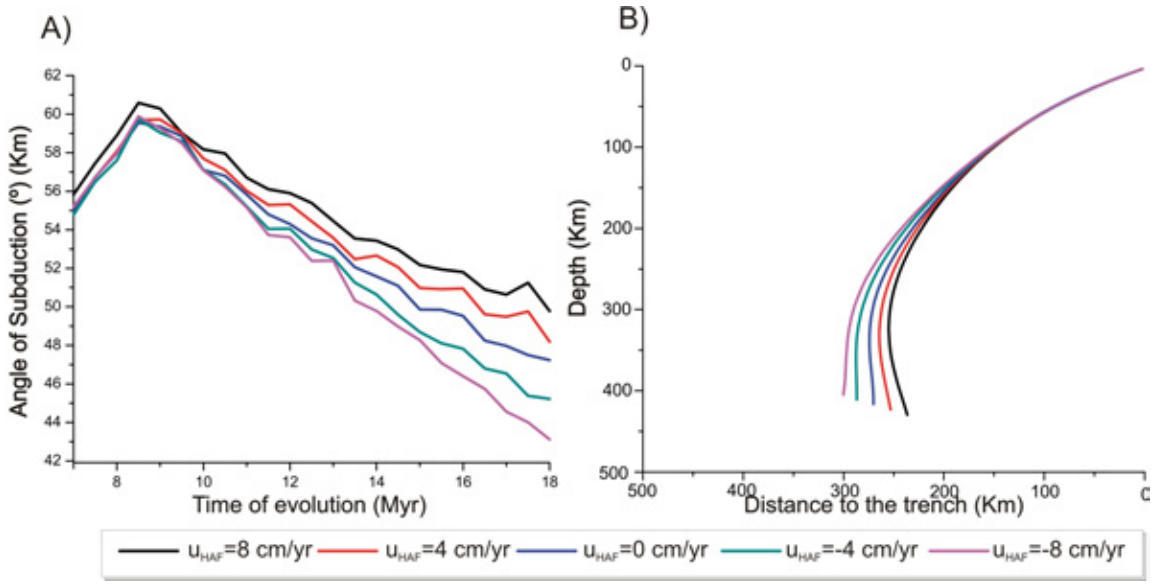

Figure 3: Results for five different simulations in which the sense and velocity of the AHF is varied (negative velocities indicate that flow is directed to the right). In the initial state the upper plate is 20 Myr old and the lower plate 40 Myr old for all models. A) Evolution of the angle of subduction (measured between 95 km and 195 km depths). B) Upper boundary of the slab after 18 Myr of evolution.

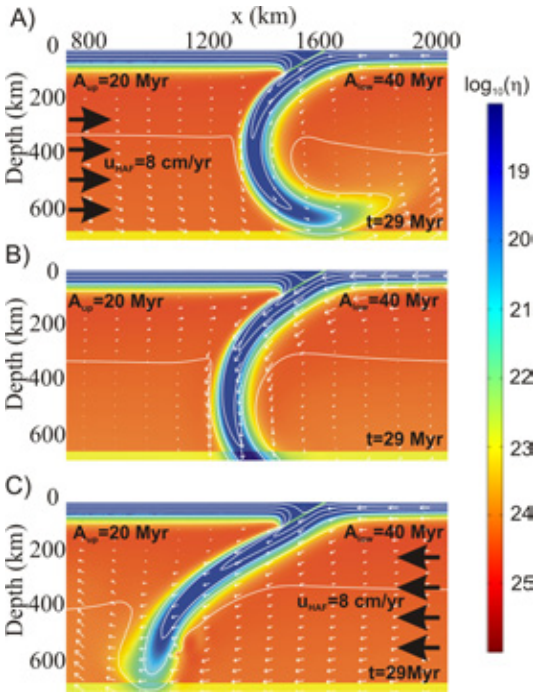

Figure 4: Three different simulations in which the upper plate is 20 Myr old and the lower plate 40 Myr old after 29 Myr of evolution. Viscosity in logarithmic scale (colormap) and contours of equal temperature every 280 K are shown. A) The HAF is directed to le right and has a velocity of 8 cm/yr. B) No HAF is imposed. A) The HAF is directed to the left and has a velocity of 8 cm/yr.

4. References

1. Barazangi, M. and Isacks, B.L., Subduction of the Nazca plate beneath Peru: evidence from spatial distribution of earthquakes, *Geophys. J. R. Astron. Soc*, **57**, 537-555 (1977)

2. Billen, M. I and Hirth, G., Newtonian versus non-newtonian upper mantle viscosity: Implications fur subduction initiation, *Geophysical Research Letters*,**32**, L19304, doi:10.1029/ 200GL023457 (2005).

3. Billen, M. I. and Hirth, G., Rheologic controls on slab dynamics, *Geochem. Geophys. Geosyst.*, **8**, Q08012, doi:101029/2007GC001597 (2007).

4. Billen, M.I. and Hirth, G., Rheologic controls on slab dynamics. *Geochem. Geophys. Geosyst.*, **8**, Q08012, doi:10.1029/2007GC001597 (2007).

5. Cruciani, C., Carminati, E. and Doglioni, C., Slab dip vs. lithosphere age: no direct function. *Earth Planet. Sci. Lett.* **238**, 298–310 (2005).

6. Cuffaro, M. and Doglioni, C., Global kinematics in deep versus shallow hotspot reference frames, *GSA Spec. Paper*, **430**, 359–374 (2007),.

7. Doglioni, C., Green, C., and Mongelli, F., On the shallow origin of hotspots and the westward drift of the lithosphere, *in* Foulger, G.R.,

Natland, J.H., Presnall, D.C., and Anderson, D.L., eds., *Plates, plumes and paradigms: Geological Society of America Special Paper* **388**, 735–749 (2005).

8. Doglioni, C., Harabaglia, P., Merlini, S., Mongelli, F., Peccerillo, A., and Piromallo, C., Orogens and slabs vs. their direction of subduction. *Earth-Science Reviews*, **45**, 167–208, (1999).

9. Gripp, A.E., and Gordon, R.G., Young tracks of hotspots and current plate velocities: *Geophys. J. Int.*, **150**, 321–364 (2002).

10. Gudmundsson, O., and Sambridge, M., A Regionalized Upper Mantle (RUM) seismic model, *J. Geophys. Res*. **103,** 7121-7136 (1998).

11. Hager, B.H., O'Connell, R.J., Subduction zone dip angles and flow driven by plate motion, *Tectonophysics*, **50**, 111-133 (1978).

12. Hirth, G., and Kohlstedt, D.L., Rheology of the ppper mantle and the mantle wedge: A view from the experimentalists, in *Inside the subduction Factory*, edited by J. Eiler, pp. 83–105 (2003), AGU, Washington, D.C.

13. Isacks, B. and Barazangi, M., Geometry of Benioff Zones: Lateral segmentation and downwards bending of the subducted lithosphere. In Talwani, M. and Pitman, W. eds., Island arc deep sea trenches and backarc basins: *American Geophysical Union Ewing Serie I*, 99-114 (1977).

14. Jarrard, R.D., Relations Among Subduction Parameters, *Rev. Geophys.* **24**, 217-284 (1986).

15. Jischke, M.C., On the dynamics of descending lithospheric plates and slip zones. *J. Geophys. Res.*, **80** 4809-4813 (1975).

16. Jordan, T.E., Isacks, B.L., Allmendinger, R.W., Brewer, J.A., Ramos V.A. and Ando, C.J., Andean tectonics related to the geometry of the subducted Nazca plate, *Geol. Soc. Am. Bull*. **94**, 341-361 (1983).

17. Kincaid, C., and Sacks, I.S., Thermal and dynamical evolution of the upper mantle in subduction zones, *J. Geophys. Res*., **102**, 12,295–12,315 (1997).

18. Kukaèka, M., and Matyska, C., Influence of the zone of weakness on dip angle and shear heating of subducted slabs, *Phys. Earth Planet. Inter*., **141**, 243–252 (2004).

19. Lallemand, S., Heuret, A., and Boutelier, D., On the relationship between slab dip, back-arc stress, upper plate absolute motion, and crustal nature in subduction zones, *Geochem. Geophys. Geosyst.*, **6**, Q09006. doi:10.1029/2005GC000917 (2005).

20. Manea, V. and Gurnis, M., Subduction zone evolution and low viscosity wedges and channels. *Earth Planet. Sci. Lett.*, **264**, 22-45 (2007).

21. Mueller, R.D., Roest W.R., Royer J.Y., Gahagan L.M. and Sclater J.G., Digital isochrons of the world's ocean floor, **J. Geophys. Res.** 102 3211-3214 (1997).

22. Stein, C.A. and Stein, S.A., A model for the global variation in oceanic depth and heat flow with lithospheric age, *Nature*, **359**, 123-129 (1992).

23. Stevenson, D. J. and Turner J. S.. Angle of subduction, *Nature*, **270**, 334–336 (1977).

24. Tovish, A., Schubert, G. and Luyendyk, B.P., Mantle flow pressure and the angle of subduction: non-Newtonian corner flows. *J. Geophys. Res.* **83** (B12), 5892–5898 (1978).

25. Tritton, D.J., Physical Fluid Dynamics . Oxford Clarendon Press, Oxford Science Publications, pp 519, (1988)

26. Wortel M.J.R., Vlaar N.J., Age-dependent subduction of oceanic lithosphere beneath western South America, *Phys. Earth Planet. Inter*. **17** 201-208 (1978).

5. Acknowledgements

This work was funded by the Spanish Plan Nacional del MEC projects CTM2006-13666-C02-02/MAR and CGL2009-13103; and funding for UCM Research Groups. This is a contribution of the Consolider-Ingenio 2010 team CSD2006-00041 (TOPO-IBERIA). Italian MIUR and Ateneo funding is acknowledged.